

Reduction of PCE and TCE by Magnetite Revisited

Johnathan D. Culpepper^a, Michelle M. Scherer^a, Thomas C. Robinson^a, Anke Neumann^b,
David Cwiertny^a, and Drew E. Latta^{a*}

^a Department of Civil and Environmental Engineering, The University of Iowa, Iowa City, IA 52242 USA
E-mail:drew-latta@uiowa.edu Tel: +1-319-936-0034

^b School of Engineering, Newcastle University, Newcastle upon Tyne, NE1 7RU, UK.

Abstract

Here we revisit whether the common mixed-valent Fe mineral, magnetite, is a viable reductant for the abiotic natural attenuation of perchloroethylene (PCE) and trichloroethylene (TCE) in anoxic groundwater plumes. We measured PCE and TCE reduction by stoichiometric magnetite as a function of pH and Fe(II) concentration. In the absence of added Fe(II), stoichiometric magnetite does not reduce PCE and TCE over a three month period. When Fe(II) is added to magnetite suspensions, PCE and TCE are reduced under Fe(II) and pH conditions that appear to be controlled by the solubility of ferrous hydroxide, Fe(OH)₂(s). Reduction rates are slow with only 1 to 30% carbon products (primarily acetylene) accumulating over several months. We conducted a similar set of experiments with Fe(OH)₂(s) alone and found that, compared to in the presence of magnetite, Fe(OH)₂(s) reduces PCE and TCE only at Fe(II) concentrations that are too high (≥ 13 mM, 726 mg/L) to be representative of natural aquifer conditions. Our results suggest that magnetite present in aquifer sediments alone is unlikely to reduce PCE and TCE sufficiently fast to contribute to natural attenuation of PCE and TCE. The lack of compelling evidence for PCE and TCE reduction by magnetite raises important questions regarding the current application of using magnetic susceptibility as a potential indicator for abiotic natural attenuation. Dynamic conditions and high Fe(II) concentrations that favor active precipitation of minerals, such as Fe(OH)₂(s) in the presence of magnetite (or other Fe minerals), however, may lead to PCE and TCE reduction that could help attenuate PCE and TCE plumes.

Environmental significance

We present evidence that suggests magnetite alone is unlikely to reduce PCE and TCE fast enough to significantly contribute to the natural attenuation of PCE and TCE in contaminated aquifer plumes. Under reducing conditions where high concentrations of ferrous iron may be present, however, active precipitation of metastable phases in the presence of magnetite (or other Fe minerals) may contribute to abiotic natural attenuation of PCE and TCE.

Submitted to *Environmental Science: Processes and Impacts*

Revised Manuscript

24 August 2018

40 Introduction

41 Perchloroethene (PCE) and trichloroethene (TCE) are chlorinated ethenes that were used at
42 thousands of industrial and commercial facilities as cleaning and metal degreasing
43 solvents.^{1,2} For decades, PCE and TCE have been, and continue to be, the most prevalent
44 priority pollutants in groundwater at hundreds of sites and a major concern for the
45 environment and human health.³⁻⁷ Despite extensive cleanup efforts costing billions of
46 dollars, PCE and TCE are still detected at many groundwater sites at concentrations above
47 regulatory limits.^{4,8,9} Recent concerns regarding energy consumption and carbon emissions
48 have made it even more critical to assess whether it is feasible for site managers to rely on
49 natural biological, chemical, and physical processes (i.e., natural attenuation) to remediate
50 chlorinated ethene plumes.¹⁰

51 Biological natural attenuation of PCE and TCE via reductive dechlorination has been
52 extensively studied. These investigations have resulted in several tools that can be used to
53 provide lines of evidence for biological natural attenuation including methods for
54 determining the numbers of *Dehalococcoides sp. (Dhc)* bacteria, vinyl chloride reductase
55 gene copy numbers (*vcrA*),¹¹⁻¹⁴ and compound-specific isotope analysis of PCE and TCE.^{15,16}
56 In addition, significant evidence has accumulated for biotic oxidation of chlorinated ethenes
57 in aerobic plumes,^{17,18} and there are hints that anaerobic oxidation may also occur coupled
58 to metal reduction.¹⁹ There still remains significant uncertainty, however, about how much
59 abiotic reduction reactions, such as reduction by ferrous iron (Fe(II)) bearing minerals,
60 natural organic matter, and reduced sulfur species contribute to natural attenuation.

61 Of the abiotic natural attenuation processes, reduction by Fe(II)-containing minerals has
62 been discussed as a potentially promising degradation pathway for chlorinated solvents for
63 over two decades.²⁰⁻²³ Abiotic PCE and TCE degradation remains of significant interest
64 largely because abiotic reduction most often occurs by reductive elimination with acetylene
65 observed as the primary end-product. Acetylene is a preferred end-product because it is
66 benign and avoids the dichloroethene and vinyl chloride stall that commonly occurs with
67 biotic reductive dechlorination pathways.²⁰⁻²⁴

68 Of the Fe(II)-containing minerals, magnetite (Fe₃O₄), a common mixed-valent Fe mineral,
69 has been suggested to be responsible for chlorinated ethene attenuation at some field
70 sites²⁴⁻²⁶ despite slow rates of reduction by magnetite observed in laboratory
71 experiments.^{24,27-29} Indeed, the promise of magnetite as a reductant for chlorinated ethenes
72 has recently led some to suggest that high magnetic susceptibility of aquifer sediments
73 could be used as a potential indicator for abiotic natural attenuation at a site.²⁵ Such proxy
74 methods are desirable due to the difficulty in measuring biologically labile products such as
75 acetylene. We also note that more recent evidence alternatively implicates an oxidative
76 abiotic pathway^{30,31} based on a Fenton-like process involving OH radical in chlorinated
77 ethene degradation by pyrite (FeS₂) in the presence of oxygen.

78 Here we revisit whether the common mixed-valent Fe mineral, magnetite, is a viable
79 reductant to contribute to abiotic natural attenuation of PCE and TCE in anoxic groundwater
80 plumes. Our results suggest that magnetite present in aquifer sediments, alone, is unlikely
81 to reduce PCE and TCE sufficiently fast to contribute to natural attenuation of PCE and TCE
82 in anoxic plumes. Under dynamic conditions that result in active precipitation of minerals
83 such as Fe(OH)₂(s), however, PCE and TCE may be reduced sufficiently fast to help attenuate
84 PCE and TCE plumes.

85 **Materials and Methods**

86 **Chemicals**

87 Tetrachloroethylene (PCE, $\geq 99\%$) and trichloroethylene (TCE, $\geq 99\%$) were purchased from
88 Sigma-Aldrich. Non-chlorinated C_2 gases were used from a certified mixture containing 2.0%
89 ethane, 1.97% ethylene and 1.9% acetylene mixture in N_2 (Praxair). Hexanes and methanol
90 (Fisher Scientific) were pesticide residue grade and ACS reagent grade $\geq 99.8\%$, respectively.
91 PCE and TCE (24, 250 & 500) mM stock solutions were gravimetrically prepared in N_2 -
92 sparged methanol, sealed with viton septa and stored in a glovebox.

93 All deionized water was deoxygenated by purging with N_2 and stored for 24 hours in an
94 anoxic glovebox (93% N_2 /7% H_2) before being used in any experiments. Buffer solutions of
95 10 mM 3-(N-Morpholino)propanesulfonic acid (MOPS, RPI Corp.) buffer solution, or 10 mM
96 Piperazine-N,N'-bis(3-propanesulfonic acid) (PIPES, GFS Chemicals) with 10 mM sodium
97 chloride (NaCl) background electrolyte were prepared. All pH adjustments were done with
98 deoxygenated hydrochloric acid (HCl) or sodium hydroxide (NaOH).

99 Ferrous chloride stock solutions (~ 1.4 M $FeCl_2 \cdot 4H_2O$) were further purified by adjusting
100 the pH to ~ 4.5 and filtering to remove any Fe(III) precipitates.

101

102 **Magnetite synthesis**

103 Magnetite was synthesized using iron chloride salts following the method used as previously
104 described.^{32,33} Briefly, 0.1 M ferrous chloride ($FeCl_2 \cdot 4H_2O$) and 0.2 M ferric chloride
105 ($FeCl_3 \cdot 6H_2O$) solutions were prepared in deoxygenated deionized water within the glovebox.
106 Both solutions were combined. The mixture was vigorously stirred and titrated using 10 M
107 NaOH to set the pH between 10.0 and 11.5. The magnetite suspension was sealed and left
108 overnight before filtering. The minerals were removed from the glovebox in a sealed vessel
109 and freeze-dried. Freeze dried minerals were ground with a mortar and pestle and sieved
110 through a 150-micron sieve and stored in the glovebox. With this approach, the (~ 20 nm)
111 magnetite particles have surface area values close to the previously reported 63 ± 7 m² g⁻¹
112 using N_2 -BET analysis.³³

113

114 **Mineral characterization**

115 Magnetite stoichiometries ($x = Fe^{2+}/Fe^{3+}$) were determined using previously established
116 methods.³² The first approach was by acid dissolution (x_d) of the magnetite in 5 M HCl under
117 glovebox atmosphere. Using the 1,10-phenanthroline method,^{32,34} we evaluated the Fe^{2+} and
118 total Fe concentrations to determine the stoichiometric ratio. Powder X-ray diffraction (x_{xrd})
119 was the second approach using a Rigaku MiniFlex II system equipped with a Co source.
120 Magnetite powders were mixed into two drops of glycerol to form a well-mixed paste in the
121 glovebox to avoid oxidation of the mineral during analysis. The powder X-ray diffraction
122 stoichiometries (x_{xrd}) were then derived from unit-cell dimension.³² Transmission Mössbauer
123 spectroscopy was performed with a variable temperature He-cooled system with a ⁵⁷Co
124 source. Unless otherwise noted, Mössbauer spectra were collected at 140 K. Spectra were
125 fit using the Recoil software³⁵ and procedures outlined by Gorski and Scherer.³² To prepare
126 samples and avoid oxidation, we sealed samples with Kapton tape in the glovebox. To
127 characterize minerals after reaction, we shook the reactor and filtered a 5 mL aliquot. These
128 post-reaction samples were sealed for XRD using a layer of Kapton tape over the sample to
129 prevent rapid oxidation of $Fe(OH)_2$.

130

131 Reactor design

132 Reactors were 160 mL glass serum bottles sealed with Viton fluoroelastomer septas (20 mm
133 x 8 mm depth, Wheaton) and contained 150 mL of liquid and 10 mL of headspace. All batch
134 reactors were prepared in a N₂/H₂ filled glovebox with an oxygen content below 1 ppm.
135 Each system was covered with foil, stored and mixed (~100 rpm) upside down to have the
136 headspace in contact with glass rather than the septum. Mixing reactors upside down was
137 important to minimize headspace gas loss through the septum. The desired mass of iron
138 oxides was added to the buffer solution, then the reactor pH was adjusted (when needed)
139 and the chlorinated solvent added via a spike from the stock solution. A PCE and TCE
140 concentration of 50 μM (8,291 and 6,570 μg/L of PCE and TCE, respectively) was used for
141 most experiments. Reactors contained either 10 mM MOPS (pH range of 7.5 to 8.0) and 10
142 mM NaCl or 10 mM PIPPS (pH > 8.0) and 10 mM NaCl as buffer and background electrolyte,
143 respectively.

144 In magnetite reactors containing Fe(II), bottles containing buffer and background
145 electrolyte were first spiked with Fe(II) from an 1.4 M FeCl₂ stock, and then the initial Fe(II)
146 concentration was measured. In reactors containing magnetite, magnetite was added, and
147 then the systems were titrated to the desired pH using 2.5 or 10 M NaOH. Because titration
148 of Fe(II) solutions results in a pH plateau near pH 8.0, we took care to add the same volume
149 of NaOH to reactors that were prepared as replicates. Once the pH was adjusted, a 500 μL
150 sample was collected after filtration and the final Fe(II) concentration ([Fe(II)]_f) of the filtrate
151 was determined. Reactors containing only Fe(II) were prepared as described above, but
152 without the addition of magnetite.

153

154 Analytical Procedures

155 Analyses of parent and product analytes were performed using an Agilent 6890 gas
156 chromatograph equipped with electron capture (ECD) and flame ionization (FID) detectors.
157 PCE and TCE were quantified with GC-ECD after a liquid-liquid extraction of 0.25 to 1 mL of
158 sample containing both the aqueous and solid phases added to 2 mL of hexanes. The
159 daughter products ethane, ethylene, acetylene, the dichloroethenes, and vinyl chloride
160 were detected using GC-FID. Further details on analytical methods are provided in the
161 Supporting Information.

162

163 Results and Discussion

164 Reduction of PCE and TCE by Magnetite

165 To evaluate whether magnetite reduces PCE and TCE, we measured PCE and TCE
166 reduction by stoichiometric magnetite ($x = \text{Fe}^{2+}/\text{Fe}^{3+} \approx 0.5$) over a range of pH values (7.0 –
167 8.0) and solids loading (5 – 20 g/L). In all experiments, we observed negligible loss of both
168 PCE and TCE over 140 days (**Figure 1 and Table S1 in the Supporting Information**). Further,
169 no carbon products were observed, and we were able to recover nearly all of the carbon
170 initially present in the system (recoveries were TCE: 105 ± 8% for $n = 7$; PCE: 98 ± 6% for $n =$
171 5, details in **Table S1**). We originally anticipated that magnetite stoichiometry would affect
172 the rate of PCE and TCE reduction by magnetite as we have previously observed that
173 magnetite stoichiometry strongly influenced the rates and extent of uranium, mercury, and

174 nitroaromatic compound reduction.³⁶⁻³⁸ Here, however, we observed no measurable
 175 reduction of PCE and TCE by magnetite even with stoichiometric magnetite ($x \approx 0.5$) and
 176 therefore did not further explore reduction of PCE and TCE by non-stoichiometric
 177 magnetite.

178 The complete lack of PCE and TCE
 179 reduction by stoichiometric magnetite
 180 was unexpected as PCE and TCE
 181 reduction by magnetite has been
 182 previously reported.²⁶⁻²⁹ A close look at
 183 the data, however, reveals that prior
 184 evidence for reduction of PCE and TCE
 185 by magnetite is somewhat limited.
 186 While an early study by Sivavec and
 187 Horney reported fast rates of TCE
 188 reduction by magnetite with a surface-
 189 area normalized rate coefficient (k_{SA}) of
 190 $4.5 \times 10^{-4} \text{ L m}^{-2} \text{ d}^{-1}$ (half-life of 19
 191 days),²⁸ more recent studies²⁶⁻²⁹
 192 reported about 100-fold slower rates
 193 ($k_{SA} \approx 10^{-6} \text{ L m}^{-2} \text{ d}^{-1}$) than those in
 194 Sivavec and Horney.²⁸ In addition,
 195 carbon reduction products were only
 196 reported in one study²⁹, and in that
 197 study the uncertainties on product
 198 measurements were quite large (30 –
 199 200%). Based on the high
 200 uncertainties, the authors
 201 appropriately chose not to quantify
 202 rates of reduction.²⁹ Of the other two studies, the anomalously high rate of reduction was
 203 based on TCE loss alone with no report of products²⁸ and the other study relied on chloride
 204 accumulation to indicate that reduction had occurred.²⁷ Given the rather limited
 205 observations of reduced carbon products and high uncertainties in the previously reported
 206 data, we suggest that our observation of negligible reduction of PCE and TCE by magnetite is
 207 not so surprising.

208 Despite the limited laboratory evidence for PCE and TCE reduction by magnetite,
 209 degradation rates extrapolated from fate and transport modelling of monitoring well
 210 concentrations in the field have sometimes been attributed to abiotic attenuation of
 211 chlorinated ethenes by magnetite.^{24-26,39} For example, aquifer degradation rate coefficients
 212 (k_{aquifer}) on the order of $\sim 1 \text{ yr}^{-1}$ were extrapolated from contaminated groundwater at Twin
 213 Cities Army Ammunition Plant (TCAAP) to describe chlorinated ethene plumes that were
 214 smaller than expected based on dilution.^{26,44,45} More extensive data was collected for cis
 215 and 1,1-DCE and the combination of plume attenuation beyond dilution, microcosm data
 216 showing similar degradation rates with sterile and autoclaved sediments, and the presence
 217 of magnetite in the sediments led the authors to conclude that the loss of DCE may be due
 218 to reaction with magnetite.²⁶ While this a reasonable conclusion to draw, it is not, as was
 219 noted by Ferrey et. al., the only potential explanation for their observations.²⁶

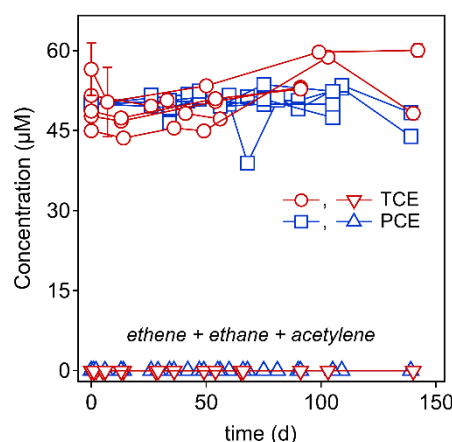


Fig. 1. PCE and TCE concentration versus time in the presence of stoichiometric magnetite ($x = \text{Fe}^{2+}/\text{Fe}^{3+} = 0.46 - 0.50$). Experimental conditions: 50 μM PCE/TCE, 10 mM MOPs/NaCl at pH 7.0, 7.5, and 8.0 for TCE reactors and pH 7.5 for PCE reactors, mass loading 5 - 20 g/L. Average carbon recoveries, TCE ($105 \pm 8\%$) for ($n = 7$), and PCE ($98 \pm 6\%$), for ($n = 5$). Error bars represent 1σ for a set of triplicate reactors (pH 8.0, 5 g/L, TCE)

220 Nevertheless, this work²⁶ is often cited as evidence for chlorinated ethene (PCE, TCE,
 221 and DCE) reduction by magnetite^{24-26,39} despite the data only being for DCEs, a need to use
 222 rate constants from batch reactors containing high Fe(II) concentrations, and the authors
 223 carefully stating that the loss of DCE *may be* due to reaction with magnetite and further
 224 research into the mechanisms of loss is needed. Collectively, the limited field and laboratory
 225 data for reduction of PCE and TCE by magnetite, and our observation of negligible reduction
 226 of PCE and TCE by magnetite, suggests that reduction by magnetite alone is unlikely
 227 responsible for field extrapolated degradation rates of PCE and TCE that have been
 228 previously attributed to magnetite. We note that there are some important differences
 229 between our experiments and aquifer plume conditions (e.g., buffers, magnetite
 230 crystallinity, flow environment, etc.). Taken together however, the existing literature and
 231 our findings provide no rigorous evidence that magnetite reduces PCE and TCE under anoxic
 232 conditions, and in fact, suggest that magnetite does not reduce PCE and TCE under a variety
 233 of conditions.

234

235 Reduction of PCE and TCE by Magnetite and Fe(II)

236 To investigate whether magnetite
 237 plus aqueous Fe(II) can abiotically
 238 degrade PCE and TCE, we
 239 measured the reduction of PCE
 240 and TCE by magnetite in the
 241 presence of Fe(II) over a range of
 242 Fe(II) concentrations and pH
 243 values (**Table S2 and S3**).

244 Consistent with previous
 245 chlorinated ethene work,^{27,40} we
 246 found that adding Fe(II) to
 247 magnetite suspensions did, in
 248 some cases, result in PCE and TCE
 249 reduction. For example, we
 250 observed measurable loss of PCE
 251 and TCE and

252 accumulation of 25% carbon products (primarily as acetylene) with 5 g/L magnetite and 9.3
 253 mM Fe(II) or 33 mM Fe(II), for PCE and TCE, respectively (**Figure 2**). Our observation of
 254 acetylene as the primary product in all reactors suggests that reductive β -elimination of PCE
 255 and TCE was likely the primary mechanism for reduction.⁴¹ Carbon recovery was higher with
 256 TCE (99 \pm 4.3%) than PCE (78%). In an attempt to better close the PCE mass balance, we
 257 measured for reductive dechlorination products, including dichloroethenes and vinyl
 258 chloride, but did not detect any. It is unclear if the mass balance loss of PCE is due to
 259 reduction to an unknown product or loss due to sorption or volatilization, however, we did
 260 observe up to 30% PCE and TCE loss in controls sampled more frequently than these
 261 reactors (**Table S1**), suggesting volatilization was likely the main contributor to loss.

262 To avoid including potential sorption and/or volatilization losses in estimated rates of PCE
 263 and TCE reduction, we quantified reduction rates based solely on accumulation of carbon
 264 reduction products (primarily acetylene). We modeled product accumulation over time
 265 using an exponential product in-growth equation (Equation 1), where P(t) is the mass of

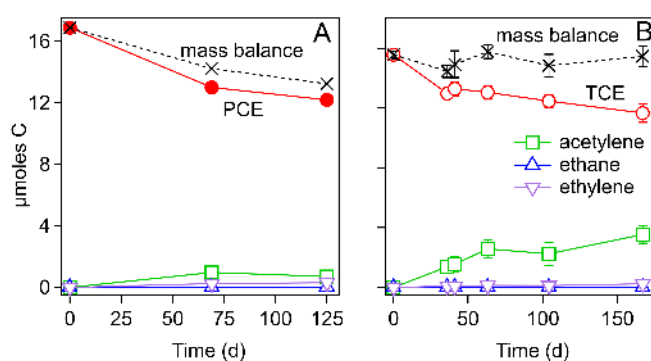


Fig. 2. Reduction of (A) PCE and (B) TCE over time with magnetite and aqueous Fe(II). Experimental conditions: (A) 54 μ M PCE, 5 g/L Fe_3O_4 (s), 33 mM Fe(II), 10 mM MOPs/NaCl, pH 7.9, single reactor. (B) 50 μ M TCE, 5 g/L Fe_3O_4 (s), 9.3 \pm 0.6 mM Fe(II), 10 mM MOPs/NaCl, pH 8, for n from 3 to 12.

266 products (in $\mu\text{moles C}$) at time t , C_0 is the initial PCE or TCE amount (in $\mu\text{moles C}$), and k_{obs} is
 267 the first-order rate coefficient. Data for total products was linearized (Equation 2), and the
 268 slope of the linearized product accumulation versus time equation was used to determine
 269 k_{obs} .

270

$$271 \quad P(t) = C_0(1 - e^{-k_{\text{obs}}t}) \quad (1)$$

272

$$273 \quad \frac{\ln\left(1 - \frac{P(t)}{C_0}\right)}{t} = -k_{\text{obs}} \quad (2)$$

274

275 First-order rate coefficients for PCE and TCE reduction determined from product
 276 accumulation varied considerably depending on the Fe(II) concentration and pH and ranged
 277 from zero to $5.2 \times 10^{-8} \text{ s}^{-1}$ (**Table S2** and **S3**).

278 We plotted k_{obs} values versus
 279 initial Fe(II) concentration and pH to
 280 explore trends in reduction rate, as
 281 we anticipated reduction rates might
 282 increase with both pH and Fe(II)
 283 concentration (**Figure 3**). Although
 284 our data are concentrated around
 285 our most common condition ($\sim \text{pH } 8$
 286 and $\sim 10 \text{ mM Fe(II)}$), there are still
 287 sufficient data to conclude that there
 288 is no clear trend with Fe(II)
 289 concentration. With pH, there is a
 290 pattern of higher pH reactors having
 291 measurable reduction ($k_{\text{obs}} > 0$), but
 292 no obvious trend of increasing rates
 293 at higher pH values. In addition, there
 294 was visual evidence from our reactors
 295 that experimental conditions had
 296 some influence on whether products
 297 were observed. More specifically, we
 298 observed a white precipitate forming
 299 in reactors in which products were
 300 observed (**Figure S1**). Given the pH
 301 and Fe(II) concentrations we used,
 302 we suspected that the white
 303 precipitate was ferrous hydroxide,
 304 $\text{Fe(OH)}_2(\text{s})$, which was confirmed by
 305 X-ray diffraction of the filtered reactor solids (**Figure S2**).

306 To quantitatively evaluate if $\text{Fe(OH)}_2(\text{s})$ precipitation was necessary for PCE and TCE
 307 reduction, we plotted k_{obs} values versus the saturation index (SI) for $\text{Fe(OH)}_2(\text{s})$ (**Figure 4**).
 308 We calculated the SI as $\log(\text{IAP}/K_{\text{sp}})$ using the initial Fe(II) concentration and an $\text{Fe(OH)}_2(\text{s})$
 309 K_{sp} of 5×10^{-15} .⁴²⁻⁴⁴ A noticeable pattern emerges with PCE and TCE reduction corresponding
 310 to conditions where the initial SI > 0 . This pattern implies that PCE and TCE reduction only

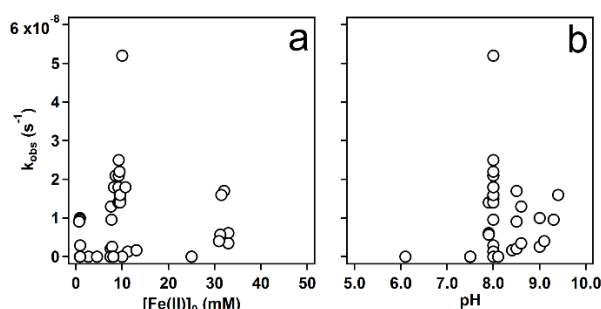


Fig. 3. Plots of k_{obs} for PCE and TCE reduction as a function of $[\text{Fe(II)}]_0$ (initial Fe(II) concentration) (a) and pH

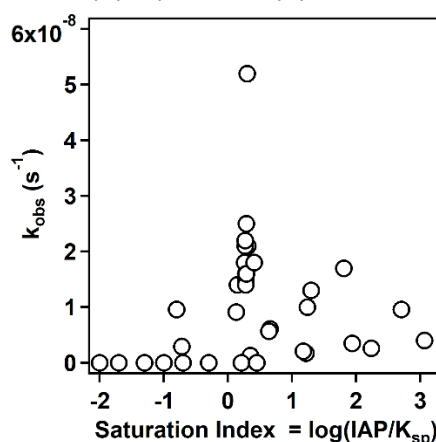


Fig. 4. Plot of k_{obs} for PCE and TCE reduction vs. the $\text{Fe(OH)}_2(\text{s})$ initial saturation index (< 0 undersaturated, 0 at saturation, > 0 oversaturated).

311 occurs under experimental conditions that are saturated (or super-saturated) with respect
 312 to $\text{Fe}(\text{OH})_2(\text{s})$ based on the amount of $\text{Fe}(\text{II})$ added and the pH value the reactor was set at.
 313 We note that after precipitation of $\text{Fe}(\text{OH})_2$, the SI is likely closer to 0. For experiments that
 314 were saturated or super-saturated,

315 93% (27 of 29) had
 316 measurable reduction products form.
 317 Conversely, for experiments that were
 318 undersaturated only 18% (2 of 11) had
 319 measurable reduction products form.

320 To better visualize the influence of
 321 $\text{Fe}(\text{OH})_2(\text{s})$ precipitation on PCE and
 322 TCE reduction, we also plotted the
 323 initial pH and $\text{Fe}(\text{II})$ concentration of
 324 these magnetite plus $\text{Fe}(\text{II})$
 325 experiments on an $\text{Fe}(\text{OH})_2(\text{s})$ solubility
 326 diagram (**Figure 5**). In Figure 5, solid,
 327 red markers indicate conditions where
 328 reduction products were observed,
 329 whereas open markers indicate
 330 conditions where no reduction
 331 products were observed. In addition,
 332 we scaled the size of the red markers
 333 to the relative amount of products
 334 formed.

335 A clear visual picture emerges
 336 highlighting that products were
 337 observed (i.e., red markers) only when
 338 $\text{Fe}(\text{II})$ concentration and pH values
 339 were such that $\text{Fe}(\text{OH})_2(\text{s})$ was
 340 expected (and visually observed) to
 341 precipitate. Of the forty experiments
 342 we conducted, thirty-six (90%)
 343 followed the trend of reduction
 344 occurring only when conditions were
 345 such that $\text{Fe}(\text{OH})_2(\text{s})$ was expected to
 346 precipitate. These results provide
 347 compelling evidence that, under our
 348 experimental conditions, precipitation
 349 of ferrous hydroxide is necessary for
 350 PCE and TCE reduction to be observed
 351 in the presence of magnetite. Note
 352 that in the presence of different buffers, such as carbonate, other minerals would likely
 353 precipitate (such as siderite or carbonate green rust).

354 Although adding $\text{Fe}(\text{II})$ to the magnetite suspensions resulted in reduction of PCE and TCE
 355 when $\text{Fe}(\text{OH})_2(\text{s})$ precipitated, the rates of reduction are still quite slow. Only 1 to 30%
 356 carbon products (primarily acetylene) accumulated over a three to five month time period.

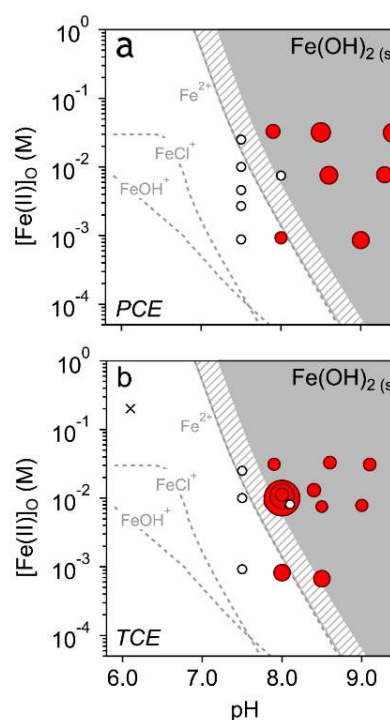


Fig. 5. $\text{Fe}(\text{OH})_2(\text{s})$ solubility diagram with magnetite plus $\text{Fe}(\text{II})$ reactor conditions overlaid for (a) PCE and (b) TCE reactors. $\text{Fe}(\text{II})$ is plotted as the initial $\text{Fe}(\text{II})$ concentration – $[\text{Fe}(\text{II})]_0$. Red markers represent PCE and TCE reactors where carbon products were observed and the markers are scaled relative to the amount of products produced (ranging up to 46%). Black open markers represent reactors where no products were observed. The grey hatched area represents a range of ferrous hydroxide solubility product K_{sp} ($[\text{Fe}(\text{OH})_2(\text{s})] = [\text{Fe}^{2+}] [\text{OH}^-]^2$) of $10^{-14.51}$ to $10^{-15.11}$.⁴²⁻⁴⁴ The grey hatched and shaded areas represent the region where $\text{Fe}(\text{OH})_2$ is expected to precipitate. Speciation diagrams were calculated with Visual MINTEQ for 10 mM Na^+ and 30 mM Cl^- to represent Cl^- added with a nominal $\text{Fe}(\text{II})$ spike of 10 mM.

357 Surface-area normalized first-order rate coefficients (k_{SA}) estimated from carbon product
358 accumulation ranged from 3.7×10^{-7} to $1.5 \times 10^{-5} \text{ L m}^{-2} \text{ d}^{-1}$, corresponding to half-lives ($t_{1/2}$)
359 ranging from 0.42 to 17 years (**Table S2 and S3**). These rates are much slower than those for
360 TCE reported by Sivavec in experiments conducted at pH 6.0 and 200 mM Fe(II) with 217 g/L
361 magnetite ($t_{1/2} \sim 3 \text{ d}$).⁴⁰ We attempted to reproduce the experimental conditions used in
362 the Sivavec patent but observed no measurable TCE reduction (**Figure S3**). One possible
363 explanation for the rapid TCE reduction observed by Sivavec is that the conditions may have
364 led to formation of green rust, which has been shown to reduce PCE and TCE.⁴⁵ Note that
365 our replication of Sivavec's conditions (marked by × in **Figure 5**) are well below ferrous
366 hydroxide saturation and therefore consistent with our finding that no reduction by
367 magnetite occurs under these conditions.
368

369 Reduction of PCE and TCE by Fe(II) and ferrous hydroxide

370 Our observation that $\text{Fe}(\text{OH})_2(\text{s})$ precipitation is necessary for PCE and TCE reduction to
 371 occur in the presence of magnetite led us to wonder whether $\text{Fe}(\text{OH})_2(\text{s})$ or even aqueous
 372 Fe(II) alone can reduce TCE. To evaluate whether $\text{Fe}(\text{OH})_2(\text{s})$ alone or aqueous Fe(II) alone
 373 could reduce TCE, we measured TCE reduction over a wide range of Fe(II) concentrations
 374 and pH values (in the absence of magnetite) and plotted the results on an $\text{Fe}(\text{OH})_2(\text{s})$
 375 solubility diagram (**Figure 6**). As
 376 expected, no reduction of PCE and TCE
 377 was observed by aqueous Fe(II)
 378 (denoted by open markers). For most
 379 conditions, no PCE and TCE reduction
 380 were observed even when $\text{Fe}(\text{OH})_2(\text{s})$
 381 had precipitated. However, at *very* high
 382 concentrations of initial Fe(II) (> 13
 383 mM, 726 mg/L) some slow PCE and TCE
 384 reduction was observed with 0.3 to
 385 13% products accumulating over a five
 386 to six month time period. First-order
 387 rate coefficients for PCE and TCE
 388 reduction determined from product
 389 accumulation for these high Fe(II)
 390 experiments (in absence of magnetite)
 391 ranged from $1.8 \times 10^{-10} \text{ s}^{-1}$ to 1.8×10^{-8}
 392 s^{-1} (**Table S4** and **S5**). We thought the
 393 high Fe(II) concentrations might have
 394 resulted in precipitation of an
 395 additional phase possibly via secondary
 396 mineral transformation of the
 397 $\text{Fe}(\text{OH})_2(\text{s})$. However, XRD and
 398 Mössbauer spectroscopy of the solids
 399 after 150 days indicated no additional
 400 phases present other than $\text{Fe}(\text{OH})_2(\text{s})$
 401 (**Figures S4** and **S5**). While these results
 402 are interesting, we would like to
 403 emphasize that the high
 404 concentrations of Fe(II) (> 13 mM, 726
 405 mg/L) make these conditions unlikely
 406 to be relevant in groundwater aquifers
 407 where Fe(II) concentrations rarely
 408 exceed 50 mg/L.⁴⁶⁻⁴⁹ Finally, we caution
 409 that we are using $\text{Fe}(\text{OH})_2$ saturation
 410 index and the plot in Figures 5 and 6 as
 411 a graphical aid to explain our data. The
 412 figures should not be used as a
 413 predictive tool because if $\text{Fe}(\text{OH})_2$ precipitates the saturation index will likely be near 0.

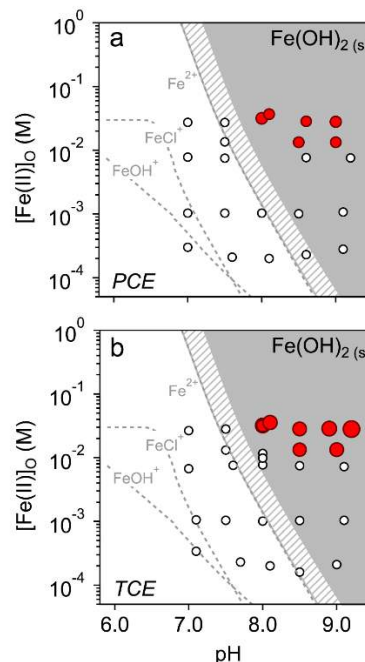


Fig. 6. $\text{Fe}(\text{OH})_2(\text{s})$ solubility diagram with aqueous Fe(II) reactors without magnetite conditions overlaid for PCE and TCE reactors. Fe(II) is plotted as the initial Fe(II) concentration – $[\text{Fe}(\text{II})]_0$. Red markers represent PCE and TCE reactors where products were observed and the markers are scaled relative to the amount of products produced (ranging up to 46%). Black open markers represent reactors where no products were observed. The grey hatched area represents a range of ferrous hydroxide solubility product K_{sp} ($[\text{Fe}(\text{OH})_2(\text{s})] = [\text{Fe}^{2+}] [\text{OH}^-]^2$) of $10^{-14.51}$ to $10^{-15.11}$.⁴²⁻⁴⁴ The grey hatched and shaded areas therefore represent the region where $\text{Fe}(\text{OH})_2$ is expected to precipitate. Speciation diagrams were calculated with Visual MINTEQ for 10 mM Na^+ and 30 mM Cl^- to represent Cl^- added with a nominal Fe(II) spike of 10 mM.

414 **Conclusions and Environmental Implications**

415 **Environmental Implications**

416 Our results, combined with previous laboratory studies,^{27,29} suggest that magnetite in
417 aquifer sediments is, on its own, unlikely to reduce PCE and TCE and contribute significantly
418 to natural attenuation of PCE and TCE in anoxic plumes. We did, however, find that
419 precipitation of ferrous hydroxide in the presence of aquifer minerals such as magnetite
420 might provide a mechanism for abiotic attenuation of chlorinated ethenes. To evaluate
421 whether PCE and TCE reduction by magnetite in the presence of ferrous hydroxide could be
422 important in natural (or engineered) attenuation strategies at contaminated sites, we scaled
423 our laboratory rate coefficients (k_{SA}) to reflect aquifer conditions (k_{field}) (example
424 calculations in **Supporting Information**). Using a field magnetite content of 1 g kg^{-1} , we
425 estimated field-scaled first-order rate coefficients (k_{field}) ranging from 0.070 to 2.8 yr^{-1} ($t_{1/2}$
426 from 0.25 to 9.9 years) (**Table S2**). These rates are comparable to both sediment microcosm
427 rates and field rates that have been attributed to abiotic degradation.^{24,26} However, in
428 nearly all of our experiments the amount of Fe(II) added exceeds typical concentrations of
429 Fe(II) in groundwater (typically $< 50 \text{ mg/L}$ or 1 mM),⁴⁶⁻⁴⁹ making the precipitation of ferrous
430 hydroxide unlikely to be relevant to field conditions. Furthermore, precipitation of ferrous
431 hydroxide is unlikely in natural aquifers due the ubiquitous presence of carbonate, making
432 siderite and ferrous hydroxy-carbonate species more likely candidates for Fe(II) precipitates.
433 Our work does, however, highlight that active precipitation of reactive Fe(II) phases may be
434 important in assessing abiotic natural attenuation.

435 The lack of compelling evidence for PCE and TCE reduction by magnetite raises important
436 questions regarding whether magnetic susceptibility of aquifer sediments is a useful
437 indicator for abiotic degradation of chlorinated ethenes by magnetite.²⁵ Recent work has
438 suggested that *in situ* magnetic susceptibility measurements might be used along with
439 chlorinated ethene concentration decreases in monitoring wells as a line of evidence for the
440 occurrence of natural attenuation by sediment magnetite in an aquifer.²⁵ Our findings,
441 however, suggest that magnetic susceptibility may not be a useful indicator for abiotic
442 natural attenuation of chlorinated ethenes by reductive elimination. While magnetite and
443 maghemite have magnetic susceptibilities of 2-3 orders of magnitude greater than the other
444 Fe oxides, making magnetic susceptibility a reasonable proxy for sediment magnetite and/or
445 maghemite content, the magnetic susceptibility of magnetite and fully-oxidized maghemite
446 are within 20% of each other.⁵⁰ The similarity between maghemite and magnetite makes
447 magnetic susceptibility measurements at the field level nearly insensitive to Fe redox
448 speciation. Furthermore, the correlation shown in Weidemier et al.²⁵ between chlorinated
449 ethene degradation and magnetic susceptibility is weak, with $r^2 = 0.18$ and a Spearman's
450 rank-order correlation coefficient of 0.41, making the correlation statistically non-significant
451 at even a 90% confidence interval (critical $p = 0.49$).

452 Our work, together with the poor mechanistic and statistical correlation between
453 magnetic susceptibility and abiotic chlorinated ethene reduction by magnetite suggests that
454 further measurements are needed to link iron mineralogy to abiotic natural attenuation.
455 Although our work suggests that magnetite is not likely to contribute significantly to abiotic
456 degradation of PCE and TCE, there is substantial laboratory evidence that other Fe(II)-
457 containing Fe minerals, such as mackinawite (FeS) and green rust, reduce chlorinated
458 ethenes much faster (see reviews by He; Fan).^{24,51} The faster PCE and TCE reduction rates

459 for mackinawite and green rust suggest that reduction by these minerals may be an
460 important degradation process in contaminated plumes. Indeed, sulfate amendments to
461 induce biological formation of mackinawite in-situ has been demonstrated in the field and in
462 the laboratory.⁵²⁻⁵⁶ Consistent with active precipitation of FeS being important for continued
463 degradation of PCE and TCE in sulfate-reducing field sites,⁵⁴ it is possible that Fe(II)
464 precipitation as Fe(OH)₂ and green rusts might occur in dynamic environments receiving a
465 constant flux of Fe(II) from dissimilatory Fe reduction, or in zones where a change in pH
466 occurs. We suggest that field screening methods for acid volatile sulfides targeting FeS⁵⁷ and
467 citrate-bicarbonate (CB) extractable Fe targeting green rusts and labile Fe(II) phases^{58,59}
468 might provide a measure of the potential for abiotic chlorinated ethene reduction by Fe(II)
469 and sulfide minerals, although further study is needed. Zones of active Fe(II) precipitation in
470 anoxic aquifer could result in PCE and TCE reduction that is sufficiently fast to help
471 attenuate PCE and TCE plumes.

472

473 **Conflicts of interest**

474 There are no conflicts to declare.

475

476 **Acknowledgements**

477 This research has been funded entirely with funds from the Strategic Environmental
478 Research and Development Program – (SERDP) project ER-2532, and an NSF – GRFP to
479 Johnathan Culpepper. The contents do not necessarily reflect the views and policies either
480 of the sponsors nor does mention of trade names or commercial products that constitute
481 endorsement or recommendation for use. The authors would like to thank Luiza Notini
482 (University of Iowa) for designing the table of contents art.

483

484 **Electronic Supplementary Information**

485 † Electronic Supplementary Information (ESI) available: See DOI: 10.1039/x0xx00000x

486

487

488 **References**

489 1. Doherty, R. E., A history of the production and use of carbon tetrachloride,
490 tetrachloroethylene, trichloroethylene and 1, 1, 1-trichloroethane in the United States: Part
491 1--historical background; carbon tetrachloride and tetrachloroethylene. *Environmental*
492 *forensics* **2000**, *1*, (2), 69-81.

493 2. Doherty, R. E., A history of the production and use of carbon tetrachloride,
494 tetrachloroethylene, trichloroethylene and 1, 1, 1-trichloroethane in the United States: part
495 2--trichloroethylene and 1, 1, 1-trichloroethane. *Environmental Forensics* **2000**, *1*, (2), 83-93.

496 3. Pankow, J. F.; Cherry, J. A., Dense chlorinated solvents and other DNAPLs in groundwater:
497 History, behavior, and remediation. **1996**.

498 4. Kueper, B. H.; Stroo, H. F.; Vogel, C. M.; Ward, C. H., *Chlorinated solvent source zone*
499 *remediation*. Springer: 2014.

- 500 5. Guyton, K. Z.; Hogan, K. A.; Scott, C. S.; Cooper, G. S.; Bale, A. S.; Kopylev, L.; Barone Jr, S.;
501 Makris, S. L.; Glenn, B.; Subramaniam, R. P., Human health effects of tetrachloroethylene:
502 key findings and scientific issues. *Environ. Health. Perspect.* **2014**, *122*, (4), 325.
- 503 6. Chiu, W. A.; Jinot, J.; Scott, C. S.; Makris, S. L.; Cooper, G. S.; Dzubow, R. C.; Bale, A. S.;
504 Evans, M. V.; Guyton, K. Z.; Keshava, N., Human health effects of trichloroethylene: key
505 findings and scientific issues. *Environ. Health. Perspect.* **2013**, *121*, (3), 303.
- 506 7. Lepom, P.; Brown, B.; Hanke, G.; Loos, R.; Quevauviller, P.; Wollgast, J., Needs for reliable
507 analytical methods for monitoring chemical pollutants in surface water under the European
508 Water Framework Directive. *J. Chromatogr. A* **2009**, *1216*, (3), 302-315.
- 509 8. Zogorski, J. S.; Carter, J. M.; Ivahnenko, T.; Lapham, W. W.; Moran, M. J.; Rowe, B. L.;
510 Squillace, P. J.; Toccalino, P. L., Volatile organic compounds in the nation's ground water and
511 drinking-water supply wells. *US Geological Survey Circular* **2006**, *1292*, 101.
- 512 9. Council, N. R., *Alternatives for managing the nation's complex contaminated*
513 *groundwater sites*. National Academies Press: 2013.
- 514 10. Council, N. R., *Contaminants in the subsurface: Source zone assessment and*
515 *remediation*. National Academies Press: 2005.
- 516 11. van der Zaan, B.; Hannes, F.; Hoekstra, N.; Rijnaarts, H.; de Vos, W. M.; Smidt, H.;
517 Gerritse, J., Correlation of Dehalococcoides 16S rRNA and chloroethene-reductive
518 dehalogenase genes with geochemical conditions in chloroethene-contaminated
519 groundwater. *Appl. Environ. Microbiol.* **2010**, *76*, (3), 843-850.
- 520 12. Lee, P. K.; Macbeth, T. W.; Sorenson, K. S.; Deeb, R. A.; Alvarez-Cohen, L., Quantifying
521 genes and transcripts to assess the in situ physiology of "Dehalococcoides" spp. in a
522 trichloroethene-contaminated groundwater site. *Appl. Environ. Microbiol.* **2008**, *74*, (9),
523 2728-2739.
- 524 13. Lu, X.; Wilson, J. T.; Kampbell, D. H., Relationship between Dehalococcoides DNA in
525 ground water and rates of reductive dechlorination at field scale. *Water Res.* **2006**, *40*, (16),
526 3131-3140.
- 527 14. Hendrickson, E. R.; Payne, J. A.; Young, R. M.; Starr, M. G.; Perry, M. P.; Fahnestock, S.;
528 Ellis, D. E.; Ebersole, R. C., Molecular analysis of Dehalococcoides 16S ribosomal DNA from
529 chloroethene-contaminated sites throughout North America and Europe. *Appl. Environ.*
530 *Microbiol.* **2002**, *68*, (2), 485-495.
- 531 15. Damgaard, I.; Bjerg, P. L.; Bælum, J.; Scheutz, C.; Hunkeler, D.; Jacobsen, C. S.; Tuxen,
532 N.; Broholm, M. M., Identification of chlorinated solvents degradation zones in clay till by
533 high resolution chemical, microbial and compound specific isotope analysis. *J. Contam.*
534 *Hydrol.* **2013**, *146*, 37-50.

- 535 16. Hunkeler, D.; Aravena, R.; Butler, B., Monitoring microbial dechlorination of
536 tetrachloroethene (PCE) in groundwater using compound-specific stable carbon isotope
537 ratios: microcosm and field studies. *Environ. Sci. Technol.* **1999**, *33*, (16), 2733-2738.
- 538 17. Mattes, T. E.; Alexander, A. K.; Coleman, N. V., Aerobic biodegradation of the
539 chloroethenes: pathways, enzymes, ecology, and evolution. *FEMS Microbiol. Rev.* **2010**, *34*,
540 (4), 445-475.
- 541 18. Findlay, M.; Smoler, D. F.; Fogel, S.; Mattes, T. E., Aerobic Vinyl Chloride Metabolism in
542 Groundwater Microcosms by Methanotrophic and Etheneotrophic Bacteria. *Environ. Sci.*
543 *Technol.* **2016**, *50*, (7), 3617-3625.
- 544 19. Bradley, P. M.; Landmeyer, J. E.; Dinicola, R. S., Anaerobic oxidation of [1, 2-¹⁴C]
545 dichloroethene under Mn (IV)-reducing conditions. *Appl. Environ. Microbiol.* **1998**, *64*, (4),
546 1560-1562.
- 547 20. Haderlein, S. B.; Pecher, K., Mediation of organic pollutant reduction by iron oxides.
548 *Abstr. Pap. Am. Chem. Soc.* **1997**, *213*, 129-GEOC.
- 549 21. Cwiertny, D. M.; Scherer, M. M., Abiotic Processes Affecting the Remediation of
550 Chlorinated Solvents. In *In Situ Remediation of Chlorinated Solvent Plumes*, Stroo, H. F.;
551 Ward, C. H., Eds. Springer New York: New York, NY, 2010; pp 69-108.
- 552 22. Vogel, T. M.; Criddle, C. S.; McCarty, P. L., Transformations of halogenated aliphatic
553 compounds. *Environ. Sci. Technol.* **1987**, *21*, (8), 722-736.
- 554 23. Kriegman-King, M. R.; Reinhard, M., Reduction of hexachloroethane and carbon
555 tetrachloride at surfaces of biotite, vermiculite, pyrite, and marcasite. In *Organic Substances*
556 *and Sediments in Water*, Baker, R., Ed. Lewis: MI, 1991; Vol. 2, pp 349-364.
- 557 24. He, Y. T.; Wilson, J. T.; Su, C.; Wilkin, R. T., Review of Abiotic Degradation of
558 Chlorinated Solvents by Reactive Iron Minerals in Aquifers. *Groundwater Monitoring &*
559 *Remediation* **2015**, *35*, (3), 57-75.
- 560 25. Wiedemeier, T. H.; Wilson, B. H.; Ferrey, M. L.; Wilson, J. T., Efficacy of an In-Well
561 Sonde to Determine Magnetic Susceptibility of Aquifer Sediment. *Groundwater Monitoring*
562 *& Remediation* **2017**, *37*, (2), 25-34.
- 563 26. Ferrey, M.; Wilkin, R.; Ford, R.; Wilson, J., Nonbiological removal of cis-
564 dichloroethylene and 1,1-dichloroethylene in aquifer sediment containing magnetite.
565 *Environ. Sci. Technol.* **2004**, *38*, (6), 1746-1752.
- 566 27. Lee, W.; Batchelor, B., Abiotic reductive dechlorination of chlorinated ethylenes by
567 iron-bearing soil minerals. 1. Pyrite and Magnetite. *Environ. Sci. Technol.* **2002**, *36*, (23),
568 5147-5154.

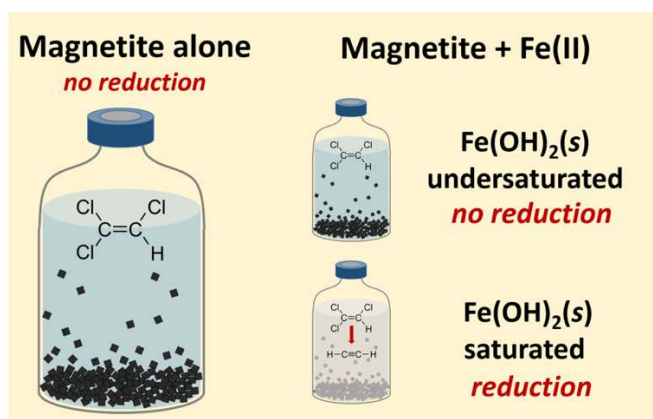
- 569 28. Sivavec, T. M.; Horney, D. P. In *Reduction of chlorinated solvents by Fe(II) minerals*,
570 213th National Meeting, San Francisco, CA, 1997; American Chemical Society: San Francisco,
571 CA, 1997; pp 115-117.
- 572 29. Liang, X. M.; Philp, R. P.; Butler, E. C., Kinetic and isotope analyses of
573 tetrachloroethylene and trichloroethylene degradation by model Fe(II)-bearing minerals.
574 *Chemosphere* **2009**, *75*, (1), 63-69.
- 575 30. Pham, H. T.; Suto, K.; Inoue, C., Trichloroethylene Transformation in Aerobic Pyrite
576 Suspension: Pathways and Kinetic Modeling. *Environ. Sci. Technol.* **2009**, *43*, (17), 6744-
577 6749.
- 578 31. Pham, H. T.; Kitsuneduka, M.; Hara, J.; Suto, K.; Inoue, C., Trichloroethylene
579 transformation by natural mineral pyrite: The deciding role of oxygen. *Environ. Sci. Technol.*
580 **2008**, *42*, (19), 7470-7475.
- 581 32. Gorski, C. A.; Scherer, M. M., Determination of nanoparticulate magnetite
582 stoichiometry by Mössbauer spectroscopy, acidic dissolution, and powder X-ray diffraction:
583 A critical review. *Am. Mineral.* **2010**, *95*, (7), 1017-1026.
- 584 33. Gorski, C. A.; Nurmi, J. T.; Tratnyek, P. G.; Hofstetter, T. B.; Scherer, M. M., Redox
585 behavior of magnetite: Implications for contaminant reduction. *Environ. Sci. Technol.* **2009**,
586 *44*, (1), 55-60.
- 587 34. Tamura, H.; Goto, K.; Yotsuyan.T; Nagayama, M., Spectrophotometric determination
588 of iron(II) with 1,10-phenanthroline in presence of large amounts of iron(III). *Talanta* **1974**,
589 *21*, (4), 314-318.
- 590 35. Lagarec, K.; Rancourt, D. G. *Recoil-Mössbauer spectral analysis software for Windows*,
591 University of Ottawa, Ottawa, ON: 1998.
- 592 36. Latta, D. E.; Gorski, C. A.; Boyanov, M. I.; O'Loughlin, E. J.; Kemner, K. M.; Scherer, M.
593 M., Influence of magnetite stoichiometry on U^{VI} reduction. *Environ. Sci. Technol.* **2012**, *46*,
594 (2), 778-786.
- 595 37. Gorski, C. A.; Nurmi, J. T.; Tratnyek, P. G.; Hofstetter, T. B.; Scherer, M. M., Redox
596 behavior of magnetite: Implications for contaminant reduction. *Environ. Sci. Technol.* **2010**,
597 *44*, (1), 55-60.
- 598 38. Pasakarnis, T. S.; Boyanov, M. I.; Kemner, K. M.; Mishra, B.; O'Loughlin, E. J.; Parkin, G.;
599 Scherer, M. M., Influence of Chloride and Fe(II) Content on the Reduction of Hg(II) by
600 Magnetite. *Environ. Sci. Technol.* **2013**, *47*, (13), 6987-6994.
- 601 39. Brown, R. A.; Wilson, J. T.; Ferrey, M., Monitored natural attenuation forum: The case
602 for abiotic MNA. *Remediation Journal* **2007**, *17*, (2), 127-137.
- 603 40. Sivavec, T. M. Composition and method for ground water remediation. U.S. Patent
604 5,750,036, May 12, 1998.

- 605 41. Arnold, W. A.; Roberts, A. L., Pathways and kinetics of chlorinated ethylene and
606 chlorinated acetylene reaction with Fe(0) particles. *Environ. Sci. Technol.* **2000**, *34*, (9), 1794-
607 1805.
- 608 42. Gustafsson, J. P. *Visual MINTEQ*, 3.0; 2011.
- 609 43. Bohnsack, G., Löslichkeit und thermodynamische Daten von Eisen(II)-Hydroxid durch
610 analytische Bestimmung des Eisens und Leitfähigkeitsmessung im System Eisen-Wasser.
611 *Berichte der Bunsengesellschaft für physikalische Chemie* **1988**, *92*, (7), 797-802.
- 612 44. Sawyer, C. N.; McCarty, P. L.; Parkin, G. F., Chemistry for environmental engineering
613 and science. **2016**.
- 614 45. Lee, W.; Batchelor, B., Abiotic reductive dechlorination of chlorinated ethylenes by
615 iron bearing soil minerals. 2. green rust. *Environ. Sci. Technol.* **2002**, *36*, (24), 5348-5354.
- 616 46. Litten, G. R., Quality of ground water used for selected municipal water supplies in
617 Iowa, 1997-2002 water years: USGS Open File Report 2004-1048. In USGS, Ed. 2004; p 36.
- 618 47. Postma, D.; Boesen, C.; Kristiansen, H.; Larsen, F., Nitrate reduction in an unconfined
619 sandy aquifer: water chemistry, reduction processes, and geochemical modeling. *Water*
620 *Resour. Res.* **1991**, *27*, (8), 2027-2045.
- 621 48. Erickson, M. L.; Barnes, R. J., Glacial sediment causing regional-scale elevated arsenic
622 in drinking water. *Groundwater* **2005**, *43*, (6), 796-805.
- 623 49. Anawar, H. M.; Akai, J.; Komaki, K.; Terao, H.; Yoshioka, T.; Ishizuka, T.; Safiullah, S.;
624 Kato, K., Geochemical occurrence of arsenic in groundwater of Bangladesh: sources and
625 mobilization processes. *J. Geochem. Explor.* **2003**, *77*, (2-3), 109-131.
- 626 50. Mullins, C., Magnetic susceptibility of the soil and its significance in soil science—a
627 review. *Eur. J. Soil Sci.* **1977**, *28*, (2), 223-246.
- 628 51. Fan, D.; Bradley, M. J.; Hinkle, A. W.; Johnson, R. L.; Tratnyek, P. G., Chemical
629 Reactivity Probes for Assessing Abiotic Natural Attenuation by Reducing Iron Minerals.
630 *Environ. Sci. Technol.* **2016**, *50*, (4), 1868-1876.
- 631 52. Kennedy, L. G.; Everett, J. W.; Gonzales, J., Assessment of biogeochemical natural
632 attenuation and treatment of chlorinated solvents, Altus Air Force Base, Althus, Oklahoma.
633 *J. Contam. Hydrol.* **2006**, *83*, 221-236.
- 634 53. Kennedy, L. G.; Everett, J. W.; Becvar, E.; DeFeo, D., Field-scale demonstration of
635 induced biogeochemical reductive dechlorination at Dover Air Force Base, Dover, Delaware.
636 *J. Contam. Hydrol.* **2006**, *88*, 119-136.
- 637 54. He, Y. T.; Wilson, J. T.; Wilkin, R. T., Transformation of reactive iron minerals in a
638 permeable reactive barrier (biowall) used to treat TCE in groundwater. *Environ. Sci. Technol.*
639 **2008**, *42*, (17), 6690-6696.

- 640 55. Whiting, K.; Evans, P. J.; Lebrón, C.; Henry, B.; Wilson, J. T.; Becvar, E., Factors
641 controlling in situ biogeochemical transformation of trichloroethene: Field survey.
642 *Groundwater Monitoring & Remediation* **2014**, *34*, (3), 79-94.
- 643 56. Evans, P. J.; Nguyen, D.; Chappell, R. W.; Whiting, K.; Gillette, J.; Bodour, A.; Wilson, J.
644 T., Factors controlling in situ biogeochemical transformation of trichloroethene: Column
645 study. *Groundwater Monitoring & Remediation* **2014**, *34*, (3), 65-78.
- 646 57. Simpson, S. L., A rapid screening method for acid-volatile sulfide in sediments. *Environ.*
647 *Toxicol. Chem.* **2001**, *20*, (12), 2657-2661.
- 648 58. Trolard, F.; Bourrie, G.; Jeanroy, E.; Herbillon, A. J.; Martin, H., Trace-Metals in Natural
649 Iron-Oxides from Laterites - a Study Using Selective Kinetic Extraction. *Geochim. Cosmochim.*
650 *Acta* **1995**, *59*, (7), 1285-1297.
- 651 59. Latta, D. E.; Boyanov, M. I.; Kemner, K. M.; O'Loughlin, E. J.; Scherer, M. M., Abiotic
652 reduction of uranium by Fe(II) in soil. *Appl. Geochem.* **2012**, *27*, (8), 1512-1524.
653
654
655
656
657
658

659 **Table of Contents Artwork**

660



661

662 Magnetite is unlikely to be as important as previously thought for abiotic reduction of PCE

663 and TCE in groundwater plumes.

Supporting Information

Reduction of PCE and TCE by Magnetite Revisited

Johnathan D. Culpepper¹, Michelle M. Scherer¹, Thomas C. Robinson¹, Anke Neumann², David Cwiertny¹, Drew E. Latta^{1*}

¹Department of Civil and Environmental Engineering, The University of Iowa, Iowa City, IA 52242 USA

²School of Engineering, Newcastle University, Newcastle upon Tyne, NE1 7RU, UK

- 12 pages, 5 figures, 5 tables -

Table of Contents

Analytical methods for chlorinated ethenes and reduction products	S2
Calculation of k_{field} and $t_{1/2 \text{ field}}$	S2
Table S1. PCE/TCE with Magnetite alone	S3
Table S2. PCE/TCE Magnetite + aqueous Fe(II) reactors with products.	S4
Table S3. PCE/TCE with Magnetite + aqueous Fe(II) reactors without products.	S5
Figure S1. Reactor Photograph	S6
Figure S2. X-Ray Diffraction spectra of a TCE reactor with Magnetite	S7
Figure S3. Reproduction of Sivavec Patent Data	S8
Table S4. PCE/TCE with aqueous Fe(II) alone and no products	S9
Table S5. PCE/TCE with aqueous Fe(II) alone, with products	S10
Figure S4. X-Ray Diffraction spectra of a TCE reactor with Fe (II) alone	S11
Figure S5. Mossbauer Spectra of white precipitate in a TCE reactor with Fe (II) alone	S12
References.	S12

Analytical methods for chlorinated ethenes and reduction products

PCE and TCE were quantified with GC-ECD after a liquid-liquid extraction of 0.25 to 1 mL of sample containing both the aqueous and solid phases added to 2 mL of hexanes. The ECD column was a Supelco Equity-5 (0.25 mm diameter x 30 m length, 0.5 μm film thickness). The carrier gas was nitrogen at a constant total flow velocities of 1.0 mL/min and a 10:1 inlet split ratio. The detector make-up gas was 95% Argon: 5% methane with flow of 30 mL/min. The oven was programmed for an initial hold of 1 min at 45 $^{\circ}\text{C}$, then 10 $^{\circ}\text{C}/\text{min}$ to 200 $^{\circ}\text{C}$. The ECD method detection limits are 0.05 $\mu\text{moles}/\text{L}$ PCE and 0.02 $\mu\text{moles}/\text{L}$ TCE for ($n = 15$).

The daughter products ethane, ethylene, acetylene, the dichloroethenes, and vinyl chloride were detected using a GC-FID. The column used was an Agilent GS-GasPro column (0.320 mm diameter x 30 m length). The carrier gas was nitrogen at a constant total flow of 1.4 mL/min and 7.5:1 inlet split ratio. The detector air flow was 450 mL/min, hydrogen flow 40 mL/min, and make-up gas type was nitrogen and a combined flow rate of 35 mL/min. The oven was set for an isothermal run of 4.5 min at 70 $^{\circ}\text{C}$. The C_2 gas analysis was done with 100 μL headspace injections into the column. The detection limits for the FID method are 1.35 $\mu\text{moles}/\text{L}$ ethane, 1.36 $\mu\text{moles}/\text{L}$ ethylene and 1.34 $\mu\text{moles}/\text{L}$ acetylene for ($n = 10$). Products with carbon number $>\text{C}_2$ were not analyzed in this study. We used Henry's law and the specific dimensionless coefficient H^{cc} to calculate dissolved C_2 gases and headspace PCE and TCE.¹ The averaged values for the H^{cc} are as follows: PCE = 1.54, TCE = 2.447, Ethane = 0.0471, and Ethylene = 0.146 and Acetylene = 1.016.¹

Calculation of k_{field} and $t_{1/2\text{-field}}$

In order to estimate field rates for PCE and TCE reduction, we have calculated a k_{field} value (in yr^{-1}) following a scheme used in Wiedemeier et al.² In that study, the authors used magnetic susceptibility data to calculate the amount of magnetite in their field samples. They used a value for the magnetic susceptibility of their field sediments of $4 \times 10^{-8} \text{ m}^3/\text{kg}$. They then used this value to derive the amount of magnetite per kg of aquifer material based on the magnetic susceptibility of magnetite ($1.117 \times 10^{-3} \text{ m}^3/\text{kg}$), the density of magnetite ($5,170 \text{ kg}/\text{m}^3$), and the bulk density of an aquifer sediment ($1,700 \text{ kg}/\text{m}^3$). Based on this calculation, estimated magnetite concentrations were $\sim 0.1 \text{ g magnetite}/\text{kg sediment}$. The maximum magnetic susceptibility that they report in their paper is $\sim 1 \times 10^{-6} \text{ m}^3/\text{kg}$. Based on their magnetic susceptibility data, one could expect masses of magnetite from 0.1 g to 10 g/kg.

Using this value, we calculated the in-aquifer 1st order decay constant (k_{aquifer}) based on our rate constant for PCE and TCE degradation:

For example, the average k_{SA} for our pH ~ 8.0 , 5 g/L magnetite, $\sim 10 \text{ mM Fe(II)}$ experiments is:
 $k_{\text{SA}} = k_{\text{obs}}/\text{SA} = 1.9 \times 10^{-8} \text{ s}^{-1}/(5 \text{ g/L} \cdot 60 \text{ m}^2/\text{g}) \cdot 3.1536 \times 10^7 \text{ s/year} = 2.0 \times 10^{-3} \text{ L m}^{-2} \text{ yr}^{-1}$

Assuming $\rho_{\text{bulk}} = 1700 \text{ kg}/\text{m}^3$, effective porosity: $\eta_e = 0.2$, that the aquifer magnetite specific surface area is consistent with that used in our study ($\text{SSA} \sim 60 \text{ m}^2/\text{g}$), and 1 g magnetite/kg sediment (m_{mag}):

$$k_{field} = \frac{m_{mag} \cdot \rho_{bulk} \cdot SSA_{mag} \cdot k_{SA}}{\eta_e} \times \frac{1m^3}{1000 L}$$

$$k_{field} = 1 \frac{\text{g magnetite}}{\text{kg sediment}} \times 1,700 \frac{\text{kg sediment}}{\text{m}^3} \times 60 \frac{\text{m}^2}{\text{g}} \times \frac{1}{0.2} \frac{\text{m}^3 \text{ sediment}}{\text{m}^3 \text{ groundwater}} \times 2.0 \times 10^{-3} \frac{\text{L}}{\text{m}^2 \cdot \text{yr}} \times \frac{1m^3}{1000 L} = 1.0 \text{ yr}^{-1}$$

We estimate $k_{field} = 1.0 \text{ yr}^{-1}$. Which gives a half-life of $\ln(2)/1 = 0.69$ year.

Table S1. PCE/TCE with Magnetite alone

[C] _o (μM) ^a	pH	Mass loading (g/L)	Stoichiometry			% loss ^b	% Products ^b	% C recovery ^b	Duration (days) ^b
			x _{ms}	x _d	x _{XRD}				
PCE									
~50 ^c	7.5	5	0.50	0.55 ± 0.02	0.53	7.0	0	88	139
~50 ^c	7.5	5	0.50	0.55 ± 0.02	0.53	7.0	0	97	139
~50 ^c	7.5	5	0.50	0.55 ± 0.02	0.53	6.9	0	101	105
~50 ^c	7.5	5	0.50	0.55 ± 0.02	0.53	6.87	0	96	105
~50 ^c	7.5	5	0.50	0.55 ± 0.02	0.53	6.87	0	106	105
TCE									
48	7.0	10	0.46	0.5 ± 0.02	n.d. ^d	-10.7	0	111	91
52	7.5	5	0.50	0.55 ± 0.02	0.53	9.9	0	93	56
45	7.5	20	0.46	0.5 ± 0.02	n.d.	-6.3	0	106	140
49	8.0	10	0.45	0.5 ± 0.02	n.d.	-7.8	0	111	91
56 ^e	8.0	5	0.50	n.d. ^d	0.52	-2.3 ^e	0	102 ^e	142 ^e
PCE Control^e									
55	7.5	0	-	-	-	30	0	70	172
TCE Control^e									
55	7.5	0	-	-	-	29	0	71	135

^a [C]_o is the initial concentration of the analyte spiked within reactor.

^b % products, % analyte loss, and % C recovery are evaluated at the final reported time point.

^c ~50 is the nominal concentration of PCE or TCE added. Calculations in ^b are based on nominal concentrations.

^d n.d. measurement not determined.

^e Averages of triplicate reactors.

TABLE S2. PCE/TCE Magnetite + aqueous Fe(II) reactors with products.

[CE] ₀ ^a μM	pH	Solids loading (g/L)	[Fe(II)] ₀ mM ^b	Saturation Index ^c	[Fe(II)] _f mM ^b	Stoichiometry		% loss ^f	% products ^f	% C recovery ^f	Duration (days)	<i>k</i> _{obs} s ⁻¹	<i>k</i> _{SA} L m ⁻² d ⁻¹	<i>k</i> _{field} ^h yr ⁻¹	<i>t</i> _{1/2 field} years
						<i>x</i> _d ^d	<i>x</i> _{xrd} ^e								
PCE															
53.7	7.9	5	32.9	0.66	29.7	0.52 ± 0.03	0.50	28	6	78	125	6.1 × 10 ⁻⁹	1.8 × 10 ⁻⁶	0.33	2.1
54.0	8.0	5	0.93	-0.72	n.d. ^g	0.54 ± 0.03	0.51	18	3	85	140	2.9 × 10 ⁻⁹	8.4 × 10 ⁻⁷	0.16	4.5
50.1	8.5	5	32.0	1.81	3.60	0.52 ± 0.03	0.50	40	16	76	125	1.7 × 10 ⁻⁸	4.9 × 10 ⁻⁶	0.91	0.76
55.3	8.6	5	7.58	1.30	1.61	0.52 ± 0.03	0.50	41	13	72	125	1.3 × 10 ⁻⁸	3.7 × 10 ⁻⁶	0.70	0.99
53.1	9.0	5	0.86	1.24	n.d.	0.54 ± 0.03	0.51	32	12	80	140	1.0 × 10 ⁻⁸	2.9 × 10 ⁻⁶	0.54	1.3
53.3	9.3	5	7.71	2.71	0.71	0.52 ± 0.03	0.50	32	10	77	125	9.6 × 10 ⁻⁹	2.8 × 10 ⁻⁶	0.52	1.3
45.8	9.4	5	31.4	3.64	3.86	0.52 ± 0.03	0.50	41	15	74	125	1.6 × 10 ⁻⁸	4.6 × 10 ⁻⁶	0.86	0.81
TCE															
55.3	8.0	5	0.82	-0.80	n.d.	0.54 ± 0.03	0.51	28	11	83	139	9.6 × 10 ⁻⁹	2.8 × 10 ⁻⁶	0.97	0.72
50.8	8.0	5	8.23	0.30	4.85	0.53 ± 0.01	0.48	24	24	99	167	1.8 × 10 ⁻⁸	5.2 × 10 ⁻⁶	1.3	0.52
51.6	8.0	5	8.54	0.31	4.23	0.53 ± 0.01	0.48	27	28	101	167	2.1 × 10 ⁻⁸	6.1 × 10 ⁻⁶	1.1	0.62
51.1	7.9	5	9.19	0.15	4.13	0.53 ± 0.01	0.48	26	18	93	167	1.4 × 10 ⁻⁸	4.0 × 10 ⁻⁶	1.2	0.59
49.7	8.0	5	9.19	0.26	5.09	0.53 ± 0.01	0.48	14	24	110	167	1.8 × 10 ⁻⁸	5.2 × 10 ⁻⁶	0.80	0.86
51.1	8.0	5	9.24	0.29	4.34	0.53 ± 0.01	0.48	31	30	99	167	2.5 × 10 ⁻⁸	7.2 × 10 ⁻⁶	0.86	0.81
49.7	8.0	5	9.24	0.27	5.2	0.53 ± 0.01	0.48	29	26	97	167	2.1 × 10 ⁻⁸	6.0 × 10 ⁻⁶	0.75	0.92
50.1	8.0	5	9.42	0.27	5.23	0.53 ± 0.01	0.48	28	30	102	167	2.2 × 10 ⁻⁸	6.3 × 10 ⁻⁶	0.86	0.81
49.8	8.0	5	9.49	0.28	5.48	0.53 ± 0.01	0.48	25	24	99	167	1.5 × 10 ⁻⁸	4.3 × 10 ⁻⁶	2.8	0.25
49.3	8.0	5	9.50	0.28	5.36	0.53 ± 0.01	0.48	22	24	102	167	1.6 × 10 ⁻⁸	4.6 × 10 ⁻⁶	0.97	0.72
50.5	8.0	5	9.52	0.28	4.98	0.53 ± 0.01	0.48	25	19	94	167	1.4 × 10 ⁻⁸	4.0 × 10 ⁻⁶	0.070	9.9
51.1	8.0	5	9.52	0.29	4.18	0.53 ± 0.01	0.48	24	20	97	167	1.6 × 10 ⁻⁸	4.6 × 10 ⁻⁶	0.31	2.3
54	8.0	5	10.0	0.30	n.d.	0.48 ± 0.03	0.56	75	46	71	168	5.2 × 10 ⁻⁸	1.5 × 10 ⁻⁵	0.091	7.6
51.2	8.0	5	10.69	0.41	4.57	0.53 ± 0.01	0.48	27	26	99	167	1.8 × 10 ⁻⁸	5.2 × 10 ⁻⁶	0.49	1.4
61.2	8.0	5	11.2	0.35	n.d.	0.48 ± 0.03	0.56	10	5	94	287	1.3 × 10 ⁻⁹	3.7 × 10 ⁻⁷	0.11	6.2
49.5	7.9	5	31.2	0.64	19.56	0.48 ± 0.03	0.45	-0.8	3	103	69	5.7 × 10 ⁻⁹	1.6 × 10 ⁻⁶	0.19	3.7
69.3	8.4	5	13.1	1.22	n.d.	0.48 ± 0.03	0.56	22	5	83	287	1.7 × 10 ⁻⁹	4.9 × 10 ⁻⁷	0.14	5.0
53.9	8.5	5	0.67	0.13	n.d.	0.54 ± 0.03	0.51	25	11	85	139	9.1 × 10 ⁻⁹	2.6 × 10 ⁻⁶	0.21	3.2
51.1	8.5	5	7.55	1.18	4.18	0.48 ± 0.03	0.45	5	2	97	125	2.1 × 10 ⁻⁹	6.0 × 10 ⁻⁷	0.97	0.72
51.5	8.6	5	32.9	1.94	3.50	0.48 ± 0.03	0.45	4.5	4	99	125	3.5 × 10 ⁻⁹	1.0 × 10 ⁻⁶	1.3	0.52
54.2	9.0	5	7.83	2.24	0.58	0.48 ± 0.03	0.45	13	3	90	125	2.6 × 10 ⁻⁹	7.5 × 10 ⁻⁷	1.1	0.62
52.2	9.1	5	30.9	3.07	1.87	0.48 ± 0.03	0.45	11	4	93	125	4.0 × 10 ⁻⁹	1.2 × 10 ⁻⁶	1.2	0.59

^a [CE]₀ = Initial chloroethylene concentration

^b [Fe(II)]_{0,f} = initial or final Fe(II) concentration, respectively

^c Saturation index = log(IAP/K_{sp}). The ion activity product (IAP) was determined with initial Fe(II) concentration and pH for each experiment. K_{sp} = [Fe²⁺] [OH⁻]² = 5 × 10⁻¹⁵.³

^d *x*_d = Magnetite Fe(II)/Fe(III) ratio from dissolution

^e *x*_{xrd} = Magnetite Fe(II)/Fe(III) ratio from x-ray diffraction.

^f % PCE or TCE loss, % Products and % Carbon recovery are taken from the final reported time point.

^g (n.d.) indicates not determined.

^h *k*_{aquifer} calculated with the assumptions: sediment magnetite content = 1 g/kg, ρ_{bulk} = 1700 kg/m³, effective porosity: η_e = 0.2, that the aquifer magnetite specific surface area is 60 m²/g.

TABLE S3. PCE/TCE with Magnetite + aqueous Fe(II) reactors without products.

[C] ₀ ^a (μM)	pH	Mass loading (g/L)	[Fe(II)] ₀ ^b (mM)	Saturation Index ^c	Stoichiometry		% loss ^f	% products ^f	% C recovery ^f	Duration (day)
					x_d ^d	x_{xrd} ^e				
PCE										
51.7	7.5	5	0.88	-1.7	0.54 ± 0.03	0.51	26	0	74	140
~50	7.5	5	2.7	-1.3	0.55 ± 0.02	0.53	10	0	90	78
~50	7.5	5	4.6	-1.0	0.39 ± 0.03	0.54	2.8	0	97	78
65	7.5	17	10.0	-0.70	0.50 ± 0.06	n.d. ^g	-24.5	0	125	91
~70	7.5	17	25.0	-0.30	0.50 ± 0.06	n.d.	-14.5	0	115	91
48.9	8.0	5	7.47	0.21	0.52 ± 0.03	0.5	6.4	0	96	125
TCE										
22 ^h	6.1	147	201 ^h	-2.0	0.43	n.d.	3.8	0	96	104
51	7.5	20	10.0	-0.70	0.50 ± 0.06	n.d.	4.0	0	96	128
50.5	7.5	20	25.0	-0.30	0.50 ± 0.06	n.d.	-2.0	0	102	128
55.2	8.1	5	8.11	0.45	0.48 ± 0.03	0.45	6	0	94	195
55.9	7.5	5	0.92	-1.7	0.54 ± 0.03	0.51	26	0	74	139

* The magnetite Fe₃O₄ mineral used in the reactor was freshly precipitated and not freeze dried.

^a [C]₀ = Initial chloroethylene concentration

^b [Fe(II)]₀ = initial Fe(II) concentration, respectively

^c Saturation index = log(IAP/K_{sp}). The ion activity product (IAP) was determined with initial Fe(II) concentration and pH for each experiment. K_{sp} = [Fe²⁺] [OH⁻]² = 5 × 10⁻¹⁵.³

^d x_d = Magnetite Fe(II)/Fe(III) ratio from dissolution

^e x_{xrd} = Magnetite Fe(II)/Fe(III) ratio from x-ray diffraction.

^f % PCE or TCE loss, % Products and % Carbon recovery are taken from the final reported time point.

^g (n.d.) indicates not determined.

^h 22 g of a mixture of freeze dried magnetite with the stoichiometry determined by a weighted average.



Figure S1. Photographs of reactors containing 5 g/L magnetite reacted with low Fe(II) (~1 mM, left) and high Fe(II) (~10 mM, right). The solids on the right contain white Fe(OH)₂(s). Conditions: 10 mM MOPS buffer at pH 8.0, and 50 μM TCE.

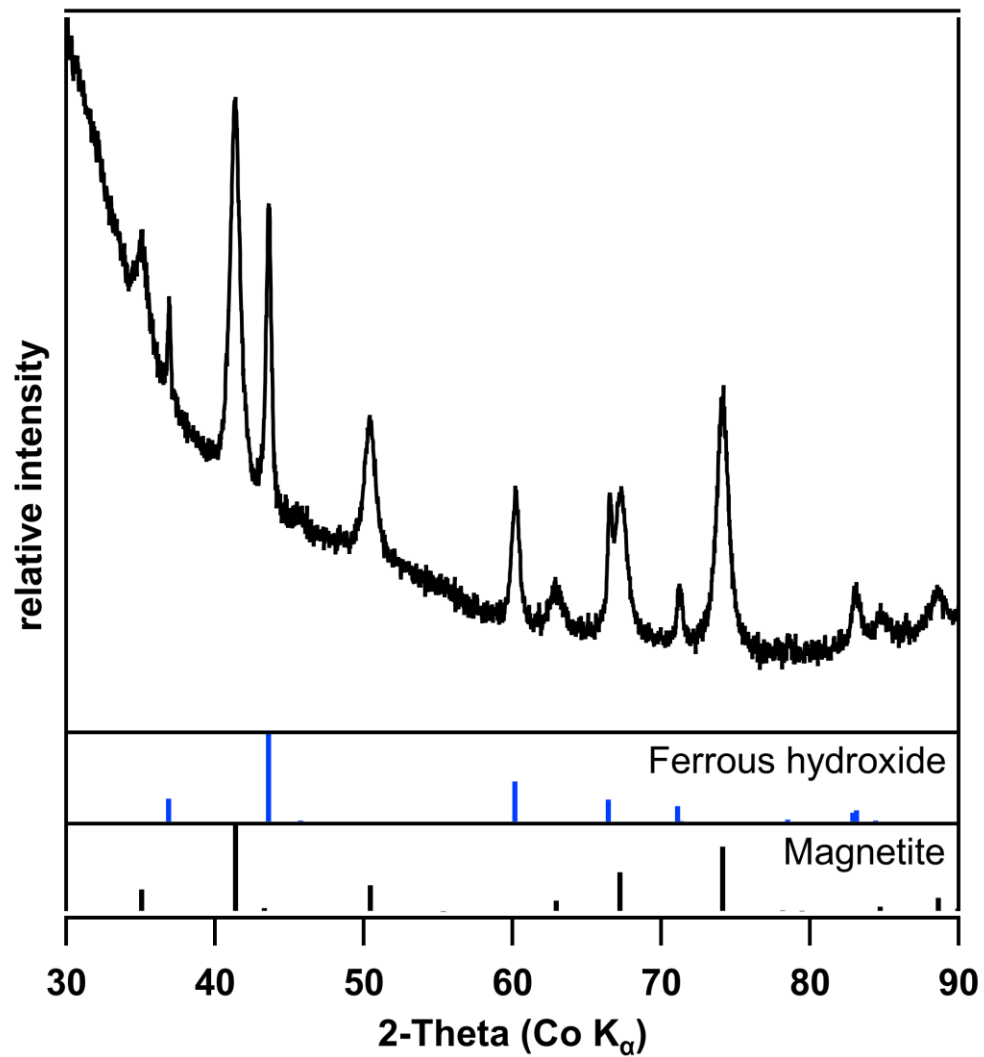


Figure S2. X-ray diffraction pattern of a TCE reactor with magnetite and Fe(II) where 30.0% products were observed after 167 days. Blue bars indicate ferrous hydroxide and black bars indicate magnetite. The background at $2\theta < 60^\circ$ is from the Kapton film used to seal the sample from air. Experimental conditions: 51 μ M TCE, 10 mM MOPs/NaCl, 9.2 mM Fe(II), pH 8.0.

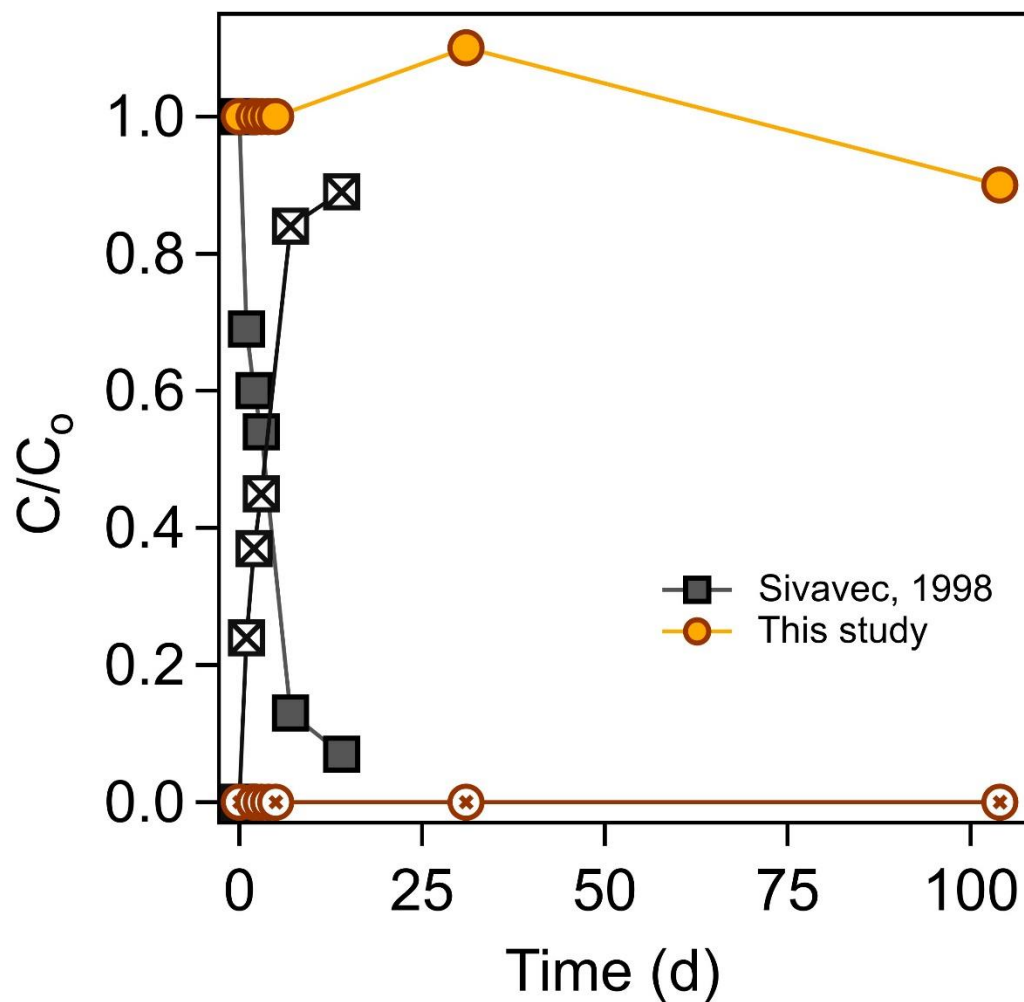


Figure S3. TCE reduction (or lack thereof) as reported in the Sivavec patent⁴ and our attempt to reproduce the data under similar conditions. **Sivavec:**⁴ 7.0 μM TCE, 217 g/L Fe_3O_4 (s), 200 mM Fe(II), pH 6.0. **This study:** 22 μM TCE, 147 g/L Fe_3O_4 (s), 201 ± 12 mM Fe(II), 10 mM MOPs/NaCl, pH 6.1

Table S4. PCE/TCE with aqueous Fe(II) alone and no products

[C] ₀ ^a (μM)	pH	[Fe(II)] ₀ ^b (mM)	Saturation Index ^c	[Fe(II)] _f ^b (mM)	% loss ^d	% products ^d	% C recovery _d	Duration (day)
PCE								
58.2	7.0	0.3	-3.0	0.16	20	0	80	138
55.2	7.0	1.03	-2.7	1.08	29.6	0	82	134
53.3	7.0	7.79	-1.8	7.52	19.1	0	81	117
50.2	7.0	27.41	-1.3	n.d. ^e	16	0	84	140
56.1	7.5	1.03	-1.6	1.06	20.4	0	70.4	134
51.2	7.5	7.52	-0.78	7.17	17.7	0	82	117
49.2	7.5	13.52	-0.52	n.d.	13	0	87	140
50.3	7.5	27.32	-0.28	n.d.	14	0	78	140
56.3	7.6	0.21	-2.3	0.21	26.1	0	74	138
57.2	8.0	1.03	-0.62	1.04	16.4	0	80	134
57	8.1	0.2	-1.2	0.18	21.9	0	78	138
53.6	8.5	1.01	0.35	1.02	16.4	0	84	134
59.1	8.6	0.23	-0.22	0.2	8.5	0	92	138
51.4	8.6	7.67	1.3	1.56	15.9	0	84	117
57	9.1	0.28	0.93	0.14	19	0	81	138
52.7	9.1	1.07	1.4	0.37	15.6	0	85	134
55.7	9.2	7.58	2.5	1.15	25.2	0	75	117
TCE								
49.4	7.0	6.71	-1.9	8.08	1	0	99	117
54.1	7.0	26.54	-1.3	n.d.	21	0	79	140
51.9	7.1	0.34	-3.0	0.33	1	0	99	138
53.3	7.1	1.06	-2.5	1.02	4.1	0	96	134
53.5	7.5	1.04	-1.6	1.08	4.1	0	96	134
52.6	7.5	13.13	-0.59	n.d.	14	0	86	140
56.9	7.5	28.16	-0.25	n.d.	16	0	84	140
53	7.6	0.23	-2.2	0.2	2.4	0	98	138
51.1	7.6	7.59	-0.70	7.64	1	0	99	117
51.7	8.0	1.01	-0.71	1.06	2.2	0	98	134
66.3	8.0	9.84	0.29	n.d.	23.5	0	77	75
152.9	8.0	9.9	0.30	n.d.	-36.6	0	33.2	75
~50 ^f	8.0	10.27	0.31	n.d.	2.3	0	98	75
~50 ^f	8.0	11.54	0.36	n.d.	3.1	0	97	75
79.9	8.0	11.64	0.37	n.d.	35	0	65	75
~50 ^f	8.0	11.79	0.37	n.d.	6.3	0	94	75
52.5	8.1	0.2	-1.2	0.24	11.1	0	89	138
53.5	8.1	7.71	0.21	6.27	5.5	0	95	117
53.8	8.5	0.16	-0.43	0.25	4.5	0	96	138
52.7	8.5	1.03	0.35	1	2.7	0	97	134
52.8	8.5	7.48	1.2	1.99	6.5	0	94	117
52.1	9.0	0.21	0.55	0.16	1.1	0	99	138
53.9	9.1	1.04	1.4	0.46	6.3	0	94	134
52	9.1	7.23	2.3	0.88	2.7	0	97	117

^a [C]₀ = Initial chloroethylene concentration

^b [Fe(II)]_{0,t} = initial or final Fe(II) concentration, respectively

^c Saturation index = log(IAP/K_{sp}). The ion activity product (IAP) was determined with initial Fe(II) concentration and pH for each experiment. $K_{sp} = [Fe^{2+}][OH^-]^2 = 5 \times 10^{-15,3}$

^d % PCE or TCE loss, % Products and % Carbon recovery are taken from the final reported time point.

^e (n.d.) indicates not determined.

^f First time point determined was not at time zero, and thus the [C]₀ is reported as a nominal concentration.

Table S5. PCE/TCE with aqueous Fe(II) alone, with products

[C] ₀ ^a (μM)	pH	[Fe(II)] ₀ ^b (mM)	Saturation Index ^c	[Fe(II)] _f ^b (mM)	% loss ^d	% products ^d	% C recovery ^d	Duration (day)	<i>k</i> _{obs} (s ⁻¹)
PCE									
50.2	8.0	31.7	0.80	1.99	27.6	2.7	75	193	1.7 × 10 ⁻⁹
54.0	8.1	36.80	1.1	33.99	23.3	1.1	77	156	8.5 × 10 ⁻¹⁰
52.7	8.5	~13.34	1.4	n.d. ^e	14	1.0	86	140	1.3 × 10 ⁻⁸
54.0	8.6	28.52	1.9	1.39	39.0	0.3	61	188	1.8 × 10 ⁻¹⁰
51.2	9.0	~13.34	2.4	n.d.	19	1.0	74	140	1.8 × 10 ⁻⁸
44.4	9.0	28.00	2.7	0.63	11.9	2.0	90	188	4.8 × 10 ⁻¹⁰
TCE									
196.9	8.0	31.62	0.80	9.39	-21.5	3.8	125	193	2.3 × 10 ⁻⁹
58.9	8.0	31.98	0.81	15.19	26.6	9	82	193	5.6 × 10 ⁻⁹
52.6	8.1	35.66	0.95	33.9	7	8	100.6	156	2.5 × 10 ⁻⁹
50.2	8.5	28.26	1.8	1.73	5	7.2	102	193	4.3 × 10 ⁻⁹
50.9	8.5	29.21	1.8	1.57	-7.9	1.2	109	193	6.6 × 10 ⁻¹⁰
56.2	8.5	~13.34	1.4	n.d.	29	6	75	140	3.0 × 10 ⁻⁹
51	8.9	28.55	2.6	0.46	7.4	9	102	193	5.7 × 10 ⁻⁹
55.6	9.0	~13.34	2.4	n.d.	24	7	83	140	5.7 × 10 ⁻⁹
51.5	9.2	28.08	3.1	0.33	23.3	13	90	193	7.7 × 10 ⁻⁹

^a [C]₀ = Initial chloroethylene concentration

^b [Fe(II)]₀ = initial Fe(II) concentration

^c Saturation index = log(IAP/K_{sp}). The ion activity product (IAP) was determined with initial Fe(II) concentration and pH for each experiment. K_{sp} = [Fe²⁺] [OH⁻]² = 5 × 10^{-15.3}

^d % PCE or TCE loss, % Products and % Carbon recovery are taken from the final reported time point. Negative loss numbers indicate higher measured TCE concentrations at the final time point than the initial time point.

^e n.d. = not determined.

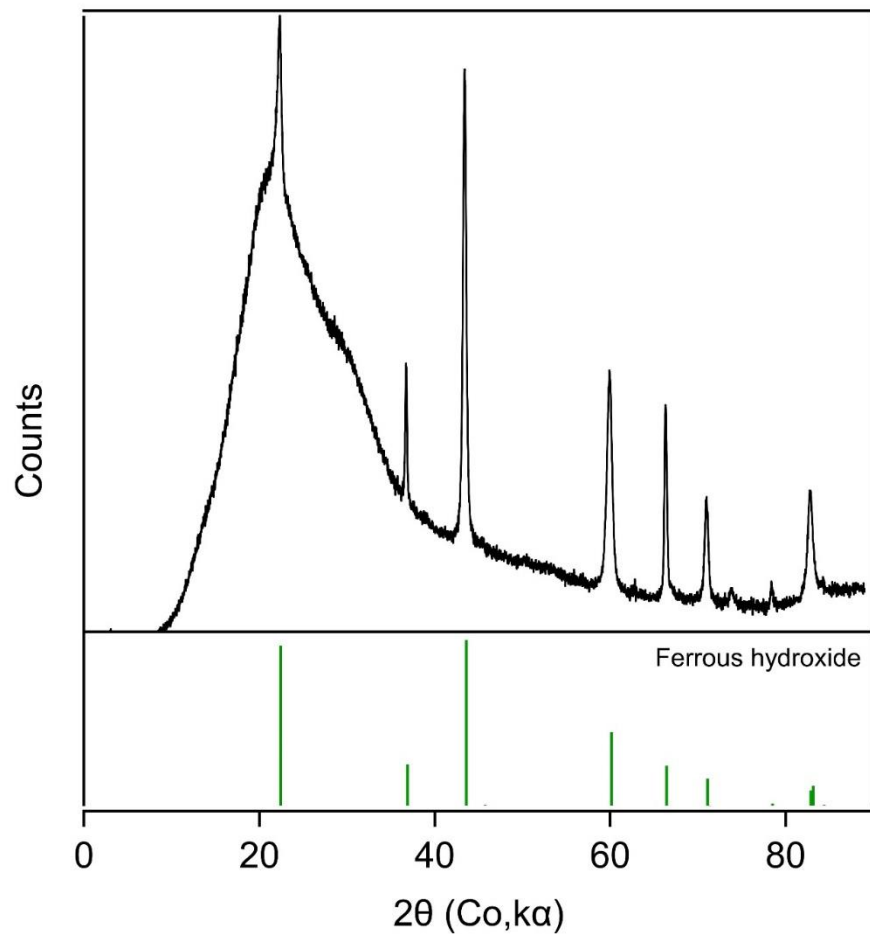


Figure S4. X-ray diffraction pattern of a TCE reactor with Fe(II) alone after 193 days where 9.0% products were observed. Light green bars indicate ferrous hydroxide. The background before 60° 2θ is due to Kapton film used to seal the sample from air. Experimental conditions: $60\ \mu\text{M}$ TCE, 10 mM MOPs/NaCl, 32 mM Fe(II), pH 8.0.

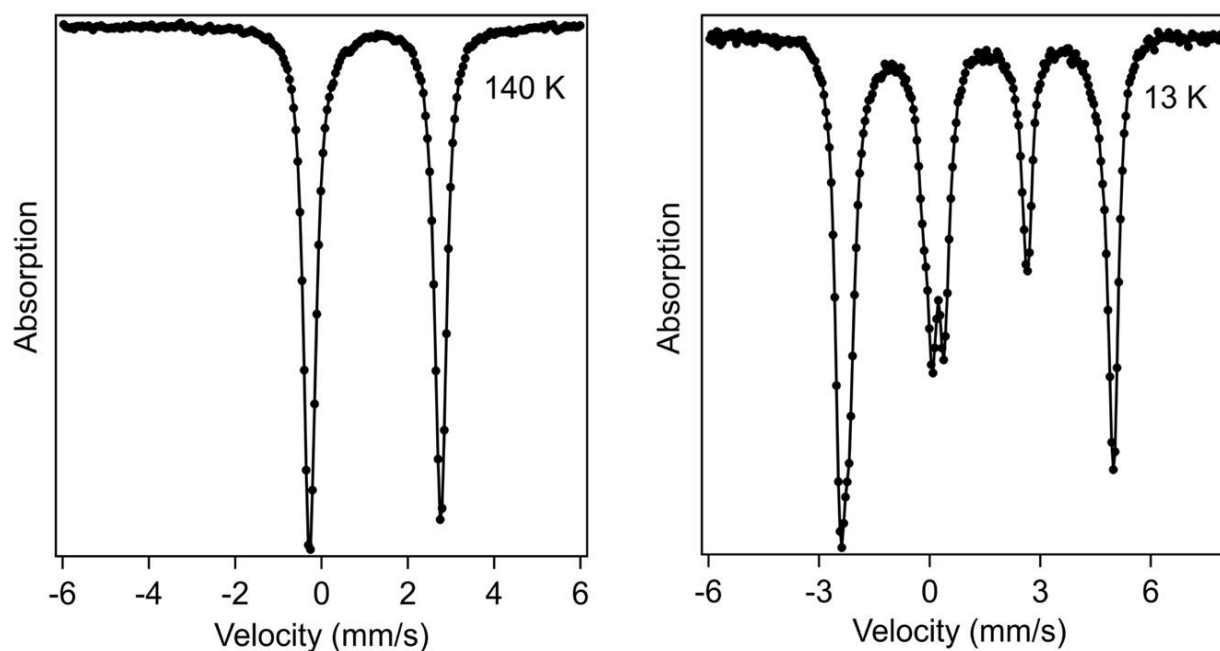


Figure S5. Mössbauer spectrum of the white precipitate in Fe(II) alone reactors after reacting with 60 μ M TCE, 10 mM MOPs/NaCl, pH 8.0 for 193 days where 9.0% products were observed. Note: 32 mM Fe(II) was the initial concentration of dissolved iron added.

References

1. Sander, R., Compilation of Henry's law constants (version 4.0) for water as solvent. *Atmospheric Chemistry and Physics* **2015**, *15*, (8), 4399-4981.
2. Wiedemeier, T. H.; Wilson, B. H.; Ferrey, M. L.; Wilson, J. T., Efficacy of an In-Well Sonde to Determine Magnetic Susceptibility of Aquifer Sediment. *Groundwater Monitoring & Remediation* **2017**, *37*, (2), 25-34.
3. Sawyer, C. N.; McCarty, P. L.; Parkin, G. F., Chemistry for environmental engineering and science. In 5th ed.; McGraw-Hill: New York, 2003.
4. Sivavec, T. M. Composition and method for ground water remediation. U.S. Patent 5,750,036, May 12, 1998.